



A Conserved Phenylalanine Residue of *Autographa Californica* Multiple Nucleopolyhedrovirus AC75 Protein Is Required for Occlusion Body Formation

Xingang Chen^{1,2}, Jian Yang^{1,2}, Xiaoqin Yang^{1,2}, Chengfeng Lei¹, Xiulian Sun^{1*} and Jia Hu^{1*}

¹ Wuhan Institute of Virology, Center for Biosafety Mega-Science, Chinese Academy of Sciences, Wuhan, China, ² College of Life Sciences, University of Chinese Academy of Sciences, Beijing, China

OPEN ACCESS

Edited by:

Julien Andreani,
IHU Mediterranee Infection, France

Reviewed by:

Peter Krell,
University of Guelph, Canada
Yves Gaudin,
Centre National de la Recherche
Scientifique (CNRS), France

*Correspondence:

Xiulian Sun
sunxl@wh.iov.cn
Jia Hu
hujia@wh.iov.cn

Specialty section:

This article was submitted to
Virology,
a section of the journal
Frontiers in Microbiology

Received: 03 February 2021

Accepted: 16 March 2021

Published: 08 April 2021

Citation:

Chen X, Yang J, Yang X, Lei C,
Sun X and Hu J (2021) A Conserved
Phenylalanine Residue of *Autographa
Californica* Multiple
Nucleopolyhedrovirus AC75 Protein Is
Required for Occlusion Body
Formation.
Front. Microbiol. 12:663506.
doi: 10.3389/fmicb.2021.663506

Autographa californica multiple nucleopolyhedrovirus (AcMNPV) *orf75* (*ac75*) is a highly conserved gene that is essential for AcMNPV propagation. However, the key domains or residues of the AC75 protein that play a role in viral propagation have not been identified. In this study, sequence alignment revealed that residues Phe-54 and Gln-81 of AC75 were highly conserved among alphabaculoviruses and betabaculoviruses. Thus, Phe-54 and Gln-81 AC75 mutation bacmids were constructed. We found that Gln-81 was not required for viral propagation, whereas mutating Phe-54 reduced budded virus production by 10-fold and impaired occlusion body formation when compared with that of the wild-type AcMNPV. Electron microscopy observations showed that the Phe-54 mutation affected polyhedrin assembly and also occlusion-derived virus embedding, whereas western blot analysis revealed that mutating Phe-54 reduced the amount of AC75 but did not affect the localization of AC75 in infected cells. A protein stability assay showed that the Phe-54 mutation affected AC75 stability. Taken together, Phe-54 was identified as an important residue of AC75, and *ac75* is a pivotal gene in budding virus production and occlusion body formation.

Keywords: *Autographa californica* multiple nucleopolyhedrovirus, AC75, Phe-54, budded virus, occlusion body

INTRODUCTION

Autographa californica multiple nucleopolyhedrovirus (AcMNPV), the type species of the genus *Alphabaculovirus* in the family *Baculoviridae*, has a circular, double-stranded DNA genome of 134 kb that codes for 154 genes (Ayres et al., 1994). AcMNPV produces two viral forms: budded viruses (BVs) and occlusion-derived viruses (ODVs) (van Oers and Vlaskovits, 2007; Rohrmann, 2019). BVs are responsible for spreading AcMNPV infection among susceptible insect cells and tissues (Blissard and Wenz, 1992), whereas ODVs initiate primary infection in the midgut epithelium of insects (Braunagel and Summers, 2007; Hodgson et al., 2007). AcMNPV genome replication and nucleocapsid assembly both occur in the nucleus. The synthesized nucleocapsids egress from the nucleus and bud from the plasma membrane to form mature BVs, whereas the retained

nucleocapsids are enveloped with intranuclear microvesicles to form ODVs that are further enclosed within polyhedrins to form occlusion bodies (OBs).

Baculovirus genome replication and transcription occur in the virogenic stroma (VS) (Young et al., 1993). The baculovirus genome is packaged into pre-assembled capsid sheaths to form mature nucleocapsids. Subsequently, a subset of the nucleocapsids egress from the nucleus to produce BVs. According to a previous report, AcMNPV nucleocapsid egress involves actin-based movement within nuclear envelope protrusions, which is coupled with localized nuclear envelope disruption and viral release into the cytoplasm (Ohkawa and Welch, 2018). Currently, several AcMNPV genes (*ac11*, *ac13*, *ac51*, *ac66*, *ac78*, *gp41*, *ac93*, *p48*, *exon0*, and *p49*) have been identified to be required for nuclear egress (Fang et al., 2007; Ke et al., 2008; McCarthy et al., 2008; Yuan et al., 2008, 2011; Tao et al., 2013, 2015; Biswas et al., 2017; Li et al., 2018; Qiu et al., 2019; Chen et al., 2020). Deletion of these genes does not affect viral genome replication and progeny nucleocapsid assembly but restrains or blocks the egress of progeny nucleocapsids from the nucleus to the cytoplasm. Recent research has shown that a group of AcMNPV proteins interact with components of the endosomal sorting complex required for transport-III complex and this complex is required for nuclear egress (Yue et al., 2018).

Nucleocapsids retained in nuclei are enveloped by intranuclear microvesicles to form ODVs and are further enclosed within the polyhedrins to form OBs (Rohrmann, 2019). The assembly and occlusion of ODVs, including intranuclear microvesicle formation, involves nucleocapsid bundles adhering to microvesicles, and subsequent wrapping of nucleocapsids by these microvesicles (Blissard and Theilmann, 2018). In previous reports, a number of AcMNPV genes (*ac11*, *ac76*, *ac93*, *odv-e25*, *p48*, and *p49*) have been shown to be involved in ODV envelopment (McCarthy et al., 2008; Yuan et al., 2008, 2011; Hu et al., 2010; Chen et al., 2012; Tao et al., 2015). Among the aforementioned genes, three genes (*ac11*, *ac93*, and *p48*) are required for both nuclear egress of the nucleocapsids and formation of intranuclear microvesicles (McCarthy et al., 2008; Yuan et al., 2008, 2011; Tao et al., 2015; Wang et al., 2019). The OBs form after the mature ODVs are embedded within polyhedrins. Then, a carbohydrate-composed outer layer and the polyhedral envelope protein (PEP) are supplemented to the surface of mature OBs (Whitt and Manning, 1988; Russell and Rohrmann, 1990), where a functional P10 protein associated with nuclear fibrillar structures is also required (Williams et al., 1989; Carpentier et al., 2008). In deletion mutants of *pep* or *p10*, OBs are irregular and fragile and no outer calyx layer is observed (Vlak et al., 1988; Li et al., 2015). Although several genes essential for OB morphogenesis have been reported, the detailed mechanism of OB morphogenesis is poorly understood.

ac75 is a highly conserved gene found in all sequenced baculovirus genomes, except *Culex nigripalpus* nucleopolyhedrovirus (CuniNPV), and *ac75* is predicted to encode a protein of 133 amino acids in length with a putative molecular mass of 15.5 kDa. AC75 localizes predominantly in the intranuclear ring zone in the late infection phase, while also exhibiting a nuclear rim distribution during the early phase

(Guo et al., 2017; Shi et al., 2017). AC75 has been reported to be associated with the envelope and nucleocapsid fractions of BVs but only with the nucleocapsid fraction of ODVs (Shi et al., 2017). In contrast, another report revealed that AC75 is associated with the nucleocapsid of BVs and with both the envelope and nucleocapsid of ODVs (Guo et al., 2017). Nevertheless, two reports both confirmed that *ac75* was required for nucleocapsid egress and intranuclear microvesicle formation (Guo et al., 2017; Shi et al., 2017).

In this study, sequence alignment revealed that Phe-54 and Gln-81 of AC75 were highly conserved among alphabaculoviruses and betabaculoviruses. We constructed Phe-54 and Gln-81 point mutation bacmids (bAc^{ac75F54S}-*ph* and bAc^{ac75Q81A}-*ph*) and evaluated the effects of these mutations on virus proliferation. The data showed that the Gln-81 mutation did not affect viral propagation, whereas the Phe-54 mutation impaired BV production, polyhedrin assembly and ODV embedding. Thus, the results showed that Phe-54 is a key residue of AC75, and *ac75* is essential for OB morphogenesis.

MATERIALS AND METHODS

Cell Lines, Viruses, Insects, and Antibodies

Sf9 cells (Invitrogen, Carlsbad, CA, United States) were cultured at 27°C in Grace's insect medium (Invitrogen) supplemented with 10% (v/v) fetal bovine serum (Gibco, Grand Island, NY, United States) and 0.1% (v/v) antibiotic-antimycotic solution (Invitrogen). The recombinant bacmids were generated from bMON14272 (Invitrogen) and maintained in *Escherichia coli* (*E. coli*) strain DH10B (Invitrogen), which also contained helper plasmids for homologous recombination and transposition. *Spodoptera exigua* (*S. exigua*) larvae were reared on an artificial diet at 28°C (Shorey and Hale, 1965).

The polyclonal antiserum of anti-AC75 was prepared in rabbits according to previously published methods (Li et al., 2018). The anti-POLH polyclonal antiserum to detect the polyhedrin protein was preserved in the laboratory. Mouse monoclonal anti-actin antibody, horseradish peroxidase (HRP)-conjugated goat anti-mouse antibody and HRP-conjugated goat anti-rabbit antibody were purchased from Proteintech (Wuhan, China).

Construction of an *ac75* Knockout Bacmid

The AcMNPV *ac75* gene was deleted using the λ red recombination system in *E. coli* BW25113 cells (containing bMON14727 and pKD46) as described previously (Datsenko and Wanner, 2000; Li et al., 2015). The *ac75*-null bacmid was constructed by replacing a 112-bp fragment of the *ac75* ORF with a chloramphenicol resistance gene (*CmR*) cassette and retaining 115 nt of the 5'-end and 175 nt of the 3'-end of the *ac75* ORF to avoid affecting transcription of neighboring genes *ac76* and *ac74*. The *ac75* knockout bacmid was verified by PCR (primer sequences are shown in **Table 1**) and termed bAc^{ac75KO}.

TABLE 1 | Primers used in this study.

Primer name	Primer sequence (5'-3') ^a
<i>ac75</i> -US-F (SacI)	<u>CGAGCTCCGCAACGAATAGAGTAAGGG</u>
<i>ac75</i> -US-R (BamHI)	<u>CGGGATCCGATAGACTTGTTCGCACAGC</u>
<i>CmR</i> -F (BamHI)	<u>CGGGATCCGTAGGCTGGAGCTGC</u>
<i>CmR</i> -R (HindIII)	<u>CCCAAGCTTCATATGAATATCCTCCTTAGTTCC</u>
<i>ac75</i> -DS-F (HindIII)	<u>CCCAAGCTTACTCAGTAGGCGACAGGTTG</u>
<i>ac75</i> -DS-R (XhoI)	<u>CCGCTCGAGCTTTGGCGTGGTCAATG</u>
<i>ph</i> -F (EcoRI)	<u>CGGAATTCACCATCTCGCAAATAAATAAG</u>
<i>ph</i> -R (SacI)	<u>CGAGCTCTGTATCGTGTTTAATACGCC</u>
<i>egfp</i> -F (SmaI)	<u>CCCCGGGATGGTGAGCAAGGGCGAGGAGC</u>
<i>egfp</i> -R (XhoI)	<u>CCGCCTGAGTCACCTTGTACAGCTCGCCATGCCGAG</u>
Dual- <i>ac75</i> -F1	<u>CCGGAGTAGCCATATTAGCCTAGTGTATGAC</u>
Dual- <i>ac75</i> -R1	<u>CAGAATTCCTTAATACGCTGGCAGTTGGTATG</u>
Dual- <i>ac75</i> -R2	<u>TTACTTATCGTCGTCATCCTTGTAAATCATAAGCTGGCAG</u> <u>TTGGTATG</u>
pFast- <i>ac75</i> -F1	<u>CGTATTAAGAATCTGCAGATATCCAGCAC</u>
pFast- <i>ac75</i> -F2	<u>TGACGACGATAAGTAAGAATCTGCAGATATCCAGCAC</u>
pFast- <i>ac75</i> -R1	<u>AATATGGCTACTCCGGAATTAATAGATCATGGAG</u>
<i>ac75</i> ^{F54S} -F	<u>AACTCAAACGAGTAGTTAATCATGAGTTAAACAATG</u>
<i>ac75</i> ^{F54S} -R	<u>TGTTTAAACTCATGTTAACTACTCGTTTGAGTTTAAAGC</u>
<i>ac75</i> ^{Q81A} -F	<u>AGTAGGCGAGCGGTTGATTTTTAATACATG</u>
<i>ac75</i> ^{Q81A} -R	<u>AAATCAACCGCTCGCCTACTGAGTTTATTAG</u>
<i>ac75</i> -F	<u>ATGTCCAATTAATGAAAACTTTTTCCACC</u>
<i>ac75</i> -R	<u>TTAATACGCTGGCAGTTGGTATGC</u>
<i>qje1</i> -F	<u>TGTGATAAACCAACCAACGAC</u>
<i>qje1</i> -R	<u>GTTAACGAGTTGACGCTTG</u>
<i>qpe38</i> -F	<u>AATGGAACAGCAGCGAATGA</u>
<i>qpe38</i> -R	<u>TGCGACGTAGTCGGAATC</u>
<i>qgp64</i> -F	<u>ACGACCTGATAGTCTCCGTG</u>
<i>qgp64</i> -R	<u>TGTAGCAATTAAGTGTGTGTC</u>
<i>qvp39</i> -F	<u>TTGCGCAACGACTTTATACC</u>
<i>qvp39</i> -R	<u>TAGACGGCTATTCCTCCACC</u>
<i>qpolh</i> -F	<u>TTAGGTGCCGTTATCAAGA</u>
<i>qpolh</i> -R	<u>GCCACTAGGTAGTTGTCT</u>
<i>q18S</i> -F	<u>TACCGATTGAATGATTTAGTGAGG</u>
<i>q18S</i> -R	<u>TACGAAACCTGTTACGACTTT</u>
pIB-F1	<u>GTCCAGTGTGGTGGAACTCTG</u>
pIB-F2	<u>CGGCGGCAGCGCGCGCGGCAGCCCCGGGATGGTG</u> <u>AGCAAGGGCGAGGAGC</u>
pIB-R	<u>TAGTGGATCCGAGCTCGGTAC</u>
pIB- <i>egfp</i> -F	<u>GAGCTCGGATCCACTAATGGTGAGCAAGG</u> <u>GCGAGGAGC</u>
pIB- <i>egfp</i> -R	<u>TTCCACCACACTGGACCTACTTGTACAGCTCGTC</u> <u>CATGCCGAG</u>
pIB- <i>ac75</i> -F	<u>GAGCTCGGATCCACTAATGTCCAATTTAATGAAAAA</u> <u>CTTTTTCCACC</u>
pIB- <i>ac75</i> -R	<u>CGCCGCTGCCGCCGCCATACGCTGGCAGTTGGTATGC</u>

^aRestriction sites and homologous sequences were underlined.

Construction of *ac75* Recombinant Bacmids

The AcMNPV *ac75* gene knockout and repair bacmids were generated as described previously (Chen et al., 2020). Briefly, the *polh* and *egfp* genes were, respectively, cloned downstream of the *polh* and *p10* gene promoters in pFastBacDual to generate

donor plasmid pFBD-*ph-egfp*. The fragment containing the *ac75* promoter and ORF was inserted into pFBD-*ph-egfp* to give the recombinant plasmid pFBD-*ph-ac75-egfp*. Subsequently, the donor plasmids pFBD-*ph-egfp* and pFBD-*ph-ac75-egfp* were transformed into *E. coli* DH10B competent cells (containing the bacmid bAc^{ac75KO} and a helper plasmid). Recombinant bacmids were selected by gentamicin and kanamycin resistance with blue-white screening and further identified by PCR (primer sequences are shown in Table 1).

The *ac75* point mutation donor plasmids were constructed using FastCloning (Li et al., 2011) and the corresponding recombinant bacmids were generated via the bac-to-bac system. For example, to generate the AC75-F54S mutant donor plasmid, the fragment was amplified by using the primer pairs *ac75*^{F54S}-F/R (sequences are shown in Table 1) and the template pFBD-*ph-ac75-egfp*. Then, 1 μL of the enzyme *DpnI* (Takara, Toyoko, Japan) was added to the PCR product (9 μL) and digested at 37°C for 1 h. The mixture was transformed into *E. coli* DH5α competent cells. The recombinant plasmid selected by gentamicin and ampicillin resistance was further validated by PCR and DNA sequencing. The donor plasmid was termed pFBD-*ph-ac75F54S-egfp*. Subsequently, the mutation plasmid pFBD-*ph-ac75F54S-egfp* was further transformed into DH10B competent cells (containing the bAc^{ac75KO} bacmid and a helper plasmid) to generate mutation bacmid bAc^{ac75F54S}-*ph* via the bac-to-bac system. The point mutation recombinant bacmid of bAc^{ac75Q81A}-*ph* was also constructed by the same methods.

Transmission Electron Microscopy and Immunoelectron Microscopy Analyses of Virus Infected Cells

Transmission electron microscopy (TEM) analysis was performed according to previous results (Qin et al., 2019). Sf9 cells infected with vAc-*ph*, vAc^{ac75F54S}-*ph*, or vAc^{ac75REP}-*ph* at an MOI of 5 were fixed with 2.5% (v/v) glutaraldehyde for 2 h and harvested at 24, 36, and 48 h post infection (p.i.). Ultrathin sections were visualized by a FEI Tecnai G² 20 TWIN TEM. For immunoelectron microscopy analysis, Sf9 cells were infected with vAc-*ph*, vAc^{ac75F54S}-*ph* or vAc^{ac75REP}-*ph* at an MOI of 5. At 48 h p.i., the cells were fixed with 1% paraformaldehyde-0.5% glutaraldehyde for 10 min at 4°C, refixed with 2% paraformaldehyde-2.5% glutaraldehyde for 1 h at 4°C and then dehydrated and embedded according to previous methods (Xu et al., 2019). Ultrathin sections were immunostained with anti-AC75 pAb (1:50) as the primary antibody. Goat anti-rabbit IgG coated with gold particles (10 nm; Sigma, Darmstadt, Germany) was used as the secondary antibody (1:50). Ultrathin sections were also visualized by using the FEI Tecnai G² 20 TWIN TEM.

Scanning Electron Microscopy (SEM), TEM, and Negative Staining Analyses of OBs

OBs were amplified and isolated from the infected larvae according to the method described by Gross et al. (Gross et al., 1994). For SEM, OBs (10⁸ OBs/mL) were loaded onto the silver paper and dried at 37°C overnight. The samples were sputter

coated with gold and examined by SEM (Hitachi SU8010). For TEM, OBs were fixed with 2.5% (v/v) glutaraldehyde for 2 h and prepared as described previously (Ji et al., 2015). Ultrathin section images were obtained by TEM (FEI Tecnai G² 20 TWIN). For negative staining analysis, 10 μ L of an OB suspension (10⁸ OBs/mL) was loaded onto a copper grid for 10 min. Filter paper was used to remove the remaining solution from the grid. Then, 10 μ L dissolution buffer was added to dissolve the OBs for 1 min. After removing the dissolution buffer, the grid was stained with 2% (w/v) phosphotungstic acid (pH 5.7) for 1 min. The grid was also examined by TEM. The number of OBs with ODVs in a field of view were counted using ImageJ software¹, and the numbers were analyzed using the Kruskal-Wallis test followed by Dunn's multiple comparison test.

Immunofluorescence Microscopy

To investigate whether AC75-F54S affected the localization of AC75, immunofluorescence assays were performed as described previously with minor modifications (Hepp et al., 2018). Briefly, Sf9 cells were seeded (4 \times 10⁵ cells/dish) on a glass dish and allowed to attach for 2 h. The cells were infected with vAc-*ph*, vAc^{ac75F54S}-*ph* or vAc^{ac75REP}-*ph* at an MOI of five and fixed with 4% paraformaldehyde for 10 min at 15, 24, and 48 h p.i. After treatment with 0.2% (v/v) Triton X-100 for 10 min and blocked with PBS containing 5% (w/v) bovine serum albumin and 0.1% (v/v) Tween-20 for 30 min, the cells were incubated with rabbit anti-AC75 polyclonal antiserum (1:500) for 1 h followed by Alexa Fluor 594 goat anti-rabbit IgG (1:1000, Invitrogen) for 1 h in the dark. Subsequently, the cell nuclei were stained with Hoechst 33258 (Beyotime, Shanghai, China). All samples were observed with a 60 \times oil-immersion objective and a PerkinElmer UltraView VOX system.

Quantitative Analysis of Viral Gene Transcription

Sf9 cells (1.0 \times 10⁶ cells/plate) were transfected in triplicate with bAc^{ac75F54S}-*ph* or bAc^{ac75REP}-*ph* bacmid DNA and collected at 24 h post-transfection (p.t.). Total cellular RNA was isolated by using RNAiso Plus (Takara). The cDNA was then synthesized using an iScript cDNA synthesis kit (Takara). qPCR was performed with five pairs of specific viral gene primers (sequences are shown in **Table 1**) by a CFX96 real-time system (Bio-Rad) under the following conditions: denaturation at 95°C for 3 min followed by 40 cycles of 95°C for 10 s, 55°C for 30 s and 72°C for 20 s. Melting curve analysis was performed at the end of each PCR assay to test specificity (control). Host 18S rRNA was selected and used as the endogenous reference.

Western Blot Analysis

Analysis of AC75 expression in cells infected with vAc^{ac75F54S}-*ph* or vAc^{ac75REP}-*ph* over the course of infection was performed by western blot. Sf9 cells were infected in triplicate with vAc^{ac75F54S}-*ph* or vAc^{ac75REP}-*ph* at an MOI of 5 and harvested at 18 and 24 h p.i. The cells were lysed on ice for 10 min in lysis buffer

(Beyotime) and centrifuged in a microcentrifuge at 16,000 \times g for 2 min. The lysates were subjected to western blot as described previously with some modifications (Xu et al., 2019). Anti-AC75 and anti-actin were used as primary antibodies. The signal was detected using a BeyoECL Plus Kit (Beyotime).

Protein Stability Analysis

Protein stability was determined by using a previously described assay (Byers et al., 2016). Briefly, Sf9 cells were infected with vAc^{ac75F54S}-*ph* or vAc^{ac75REP}-*ph* at an MOI of five and were incubated with medium containing 400 μ g/mL cycloheximide (CHX; Sigma) at 24 h p.i. The cells were harvested and lysed at the designated times, and the lysates were analyzed by western blot.

RESULTS

ac75 Is a Late Viral Gene

Transcriptomic analysis showed that three late transcription start sites are located upstream of the *ac75* translation initiation codon (Chen et al., 2013). Reverse transcription (RT)-PCR was performed in AcMNPV infected cells to confirm the temporal transcription patterns of *ac75*. The *ac75* transcripts were detected from 12 h p.i. and persisted up to 72 h p.i. (**Figure 1A**). Furthermore, western blot analysis indicated that aphidicolin inhibited AC75 expression (**Figure 1B**). These results confirmed that *ac75* was a late viral gene, implying its possible role during the late life cycle of AcMNPV.

Phe-54 Is a Key Residue of AC75

According to previous reports, *ac75* is an essential gene in the life cycle of the virus (Guo et al., 2017; Shi et al., 2017). Cells transfected with the *ac75*-null bacmid could not produce progeny BVs, which precluded analysis of the roles that AC75 plays throughout the life cycle of the virus. An InterProScan (Jones et al., 2014) and NCBI Conserved Domain Search (Marchler-Bauer et al., 2017) indicated that only a functionally unknown DUF1160 constitutes AC75, with no other annotated domains. To further investigate critical residues and functions of AC75, the sequences of AC75 homologs from 59 alphabaculoviruses and 14 betabaculoviruses were aligned by Clustal X-2.0 (Larkin et al., 2007). Residues Phe-54 and Gln-81 were found to be completely conserved among the homologs in the selected baculoviruses (**Supplementary Figure 1**). Based on this observation, we hypothesized that Phe-54 and Gln-81 from AC75 play key roles. Consequently, Phe-54 and Gln-81 point mutation bacmids (bAc^{ac75F54S}-*ph* and bAc^{ac75Q81A}-*ph*) were constructed (**Figure 2**). Sf9 cells were transfected with bAc^{ac75F54S}-*ph*, bAc^{ac75Q81A}-*ph*, bAc^{ac75REP}-*ph* or bAc-*ph* and monitored by fluorescent microscopy. There were no significant differences in the number of fluorescent cells among bacmids at 24 h p.t. (**Figure 3A**, upper panel), indicating relatively equal frequencies of transfection of these bacmids. By 72 h p.t., most of the bAc^{ac75Q81A}-*ph*-, bAc^{ac75REP}-*ph*- or bAc-*ph*-transfected cells exhibited fluorescence, whereas only a small proportion of bAc^{ac75F54S}-*ph*-transfected cells showed fluorescence (**Figure 3A**, middle panel). In addition, light

¹<https://imagej.nih.gov/ij/>

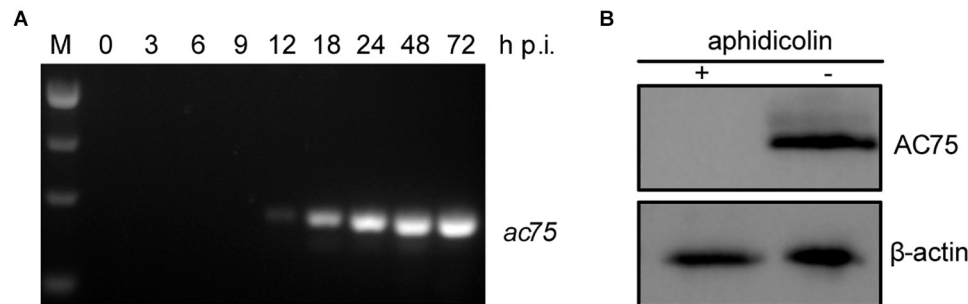


FIGURE 1 | Analyses of the transcription and expression profile of *ac75* in infected cells. **(A)** Time course analysis of *ac75* transcription. Sf9 cells infected with AcMNPV were collected at the indicated time points. Total RNA was extracted and total cDNA was obtained by reverse transcription. *ac75* was amplified with specific primer pairs by PCR. **(B)** Western blot analysis of the expression of AC75 following aphidicolin treatment. AcMNPV infected cells were treated with 5 μ g/mL aphidicolin (+) or DMSO (-) at 0 h p.i. The cells were lysed and subjected to western blot analysis with anti-AC75 and anti-actin as primary antibodies at 24 h p.i.

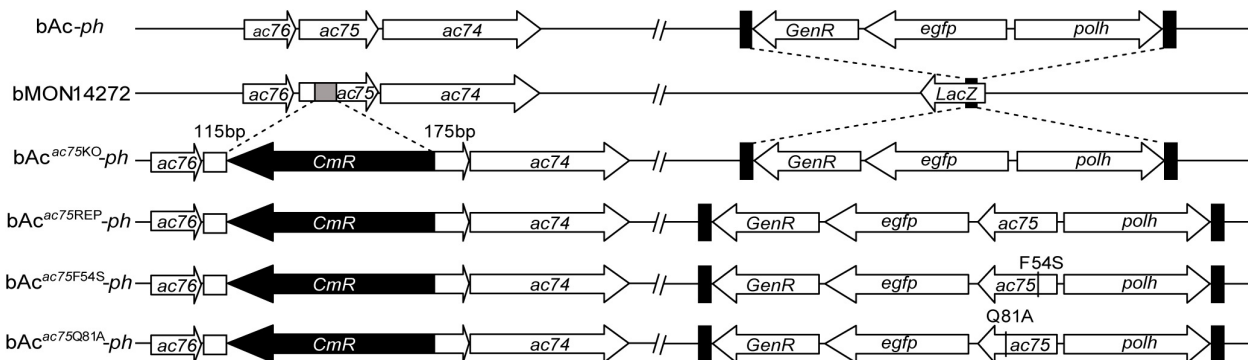


FIGURE 2 | Schematic diagram of AcMNPV, *ac75* knockout, repaired and point mutation bacmids. The 112-bp fragment of *ac75* ORF in *bMON14272* was replaced with a *CmR* cassette via homologous recombination to generate *bAc^{ac75KO}*. *bAc-ph* and *bAc^{ac75KO}-ph* were generated by inserting the *polh* and *egfp* genes into the *polh* locus of *bMON14272* and *bAc^{ac75KO}*, respectively. The *ac75*, *ac75F54S* or *ac75Q81A* controlled by the *ac75* native promoter with the *polh* and *egfp* genes were inserted into the *polh* locus of *bAc^{ac75KO}* to generate *bAc^{ac75REP}-ph*, *bAc^{ac75F54S}-ph* and *bAc^{ac75Q81A}-ph*, respectively.

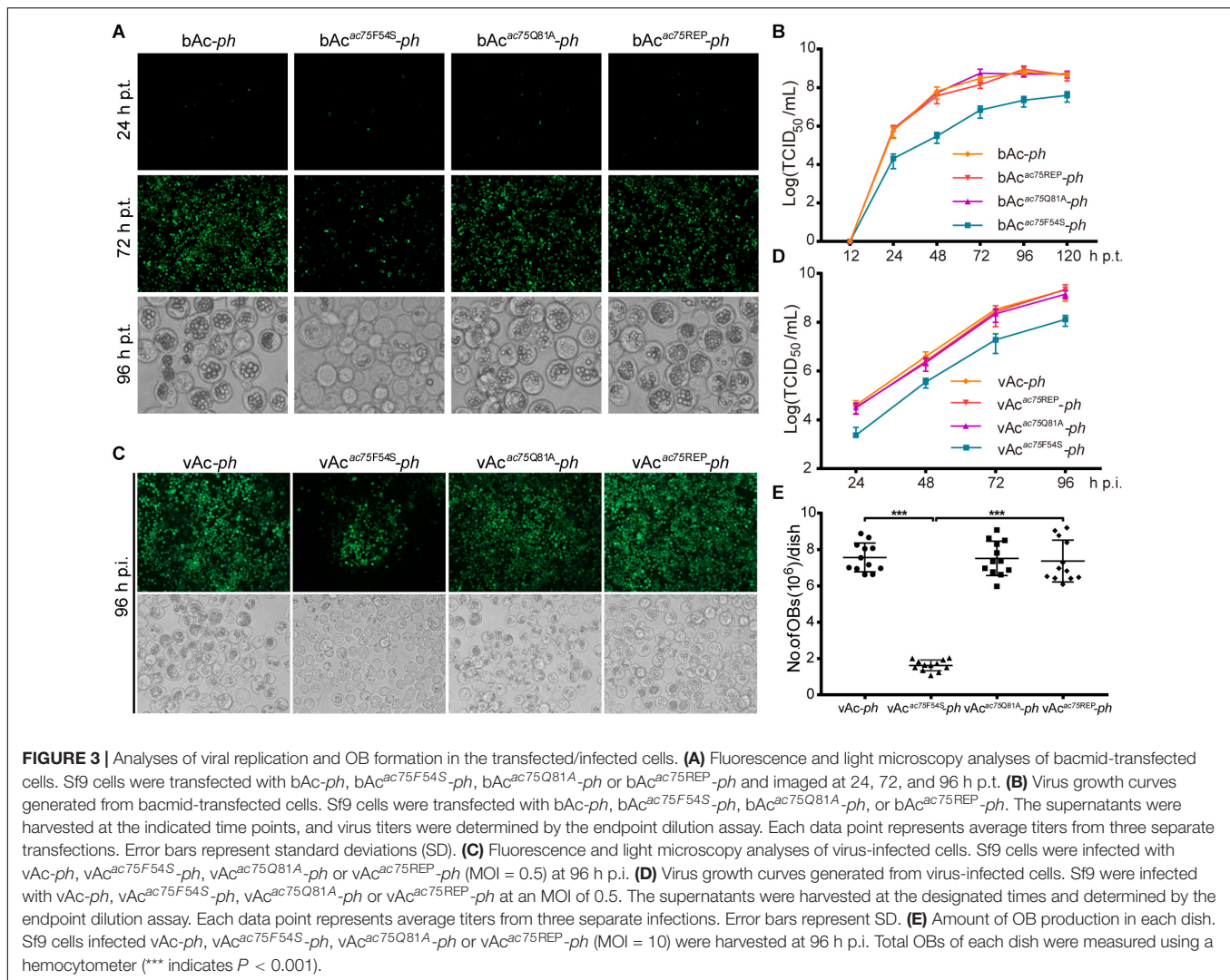
microscopy images revealed that there were fewer intracellular OBs in *bAc^{ac75F54S}-ph*-transfected cells when compared with cells transfected with the other bacmids (Figure 3A, lower panel), suggesting that the AC75-F54S mutation may also affect OB production. Furthermore, virus growth curve analysis showed that *bAc^{ac75Q81A}-ph*, *bAc^{ac75REP}-ph* and *bAc-ph* had comparable growth kinetics, whereas *bAc^{ac75F54S}-ph* produced fewer progeny BVs from 24 to 120 h p.t. (Figure 3B). Taken together, these results revealed that Phe-54 is a key residue of AC75, and the AC75-F54S mutation may affect progeny BV production and OB formation.

To further confirm the results obtained from bacmid transfection, Sf9 cells were infected with *vAc-ph*, *vAc^{ac75F54S}-ph*, *vAc^{ac75Q81A}-ph* or *vAc^{ac75REP}-ph* at an MOI of 0.5, and virus growth curve analysis was performed. At 96 h p.i., the number of fluorescent cells infected with mutant virus *vAc^{ac75F54S}-ph* was less than those infected with *vAc-ph*, *vAc^{ac75Q81A}-ph* or *vAc^{ac75REP}-ph* (Figure 3C, upper panel), and the number of OBs produced by *vAc^{ac75F54S}-ph*-infected cells was also less when compared with those cells infected with *vAc-ph*, *vAc^{ac75Q81A}-ph* or *vAc^{ac75REP}-ph* (Figure 3C, lower panel). The BV production of the *vAc^{ac75F54S}-ph* virus was reduced by 10-fold when compared

with those of *vAc-ph*, *vAc^{ac75Q81A}-ph* or *vAc^{ac75REP}-ph* from 24 to 96 h p.i. (Figure 3D). The number of OBs in cells infected with *vAc-ph*, *vAc^{ac75F54S}-ph*, *vAc^{ac75Q81A}-ph*, or *vAc^{ac75REP}-ph* at an MOI of 10 were counted. The OBs of *vAc^{ac75F54S}-ph*-infected cells from each dish were reduced by approximately eight-fold when compared with those cells infected with *vAc-ph*, *vAc^{ac75Q81A}-ph* or *vAc^{ac75REP}-ph* at 96 h p.i. ($P < 0.001$) (Figure 3E). These observations validated that the AC75-F54S mutation affected BV production and OB formation.

The AC75-F54S Mutation Affected Polyhedrin Assembly and ODV Embedding

Transmission electron microscopy was performed to further determine the effects of the AC75-F54S mutation on intranuclear structures. At 24 and 36 h p.i., *vAc^{ac75F54S}-ph*-infected cells exhibited typical baculovirus infection symptoms, including a typical VS and abundant rod-shaped nucleocapsids (Figure 4B), and ODVs with nucleocapsids (Figure 4E). As expected, *vAc-ph*- and *vAc^{ac75REP}-ph*-infected cells also showed a typical VS and normal rod-shaped nucleocapsids (Figures 4A,C), and



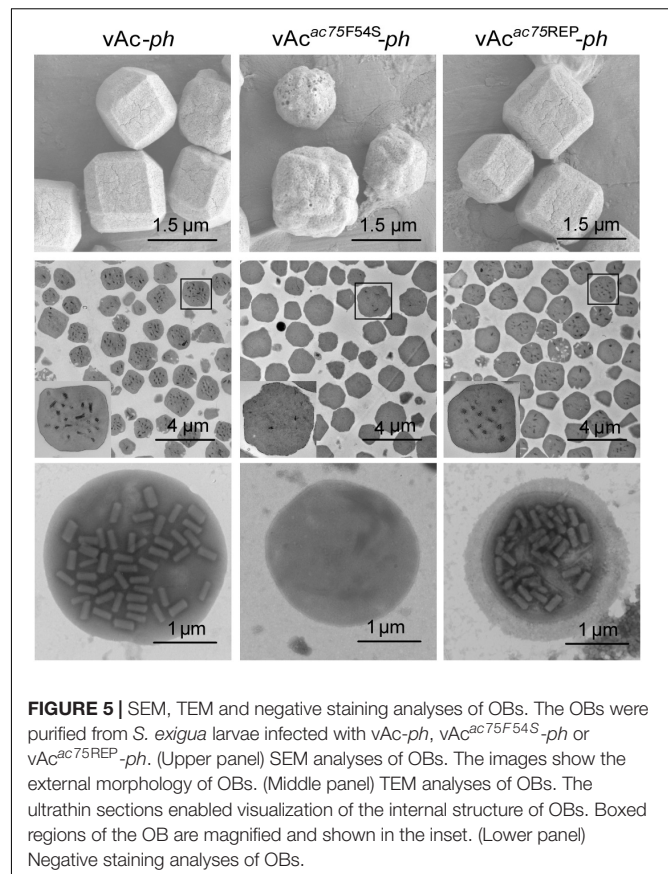
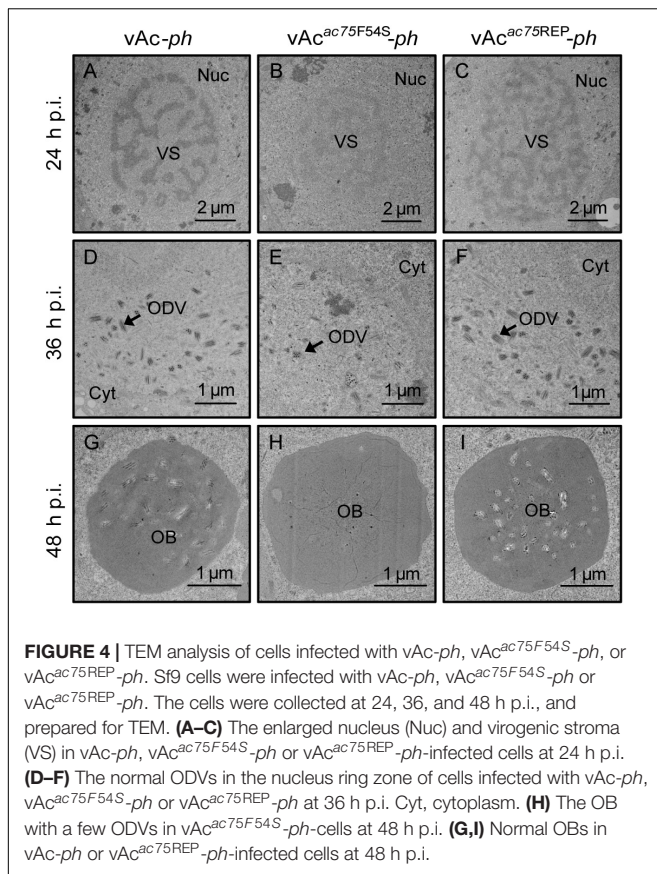
numerous ODVs (**Figures 4D,F**) at 24 and 36 h p.i. However, the OBs of vAc^{ac75F54S}-*ph*-infected cells contained fewer envelope virions (**Figure 4H**) when compared with those of vAc-*ph* and vAc^{ac75REP}-*ph*-infected cells (**Figures 4G,I**) at 48 h p.i., indicating that the AC75-F54S mutation impaired OB occlusion ODVs.

To further investigate the effects of the AC75-F54S mutation on OB morphogenesis, we performed SEM and TEM on OBs purified from vAc-*ph*-, vAc^{ac75F54S}-*ph*- or vAc^{ac75REP}-*ph*-infected *S. exigua* cadavers. SEM analysis showed that the OBs from vAc^{ac75F54S}-*ph*-infected larvae had ragged surfaces and irregular shapes, whereas the OBs of vAc-*ph* or vAc^{ac75REP}-*ph*-infected larvae had smooth surfaces and sharp edges (**Figure 5**, upper panel). TEM images showed that only a few OBs of vAc^{ac75F54S}-*ph* contained ODVs, whereas the majority of OBs of vAc-*ph* and vAc^{ac75REP}-*ph* occluded normal ODVs with multi-nucleocapsids (**Figure 5**, middle panel). Furthermore, twenty visual fields were randomly selected and analyzed, the proportion of vAc^{ac75F54S}-*ph* OBs with ODVs were only 7.8%. In addition, OBs were dissolved, negative stained and examined by TEM. Many OBs of vAc^{ac75F54S}-*ph* were empty (**Figure 5**, lower panel),

which is consistent with the observations of thin sections of OBs, whereas OBs of vAc-*ph* and vAc^{ac75REP}-*ph* contained normal single-nucleocapsids and multi-nucleocapsids (**Figure 5**, lower panel). According to these results, the AC75-F54S mutation caused aberrant polyhedrin assembly and ODV embedding during OB formation.

The AC75-F54S Mutation Did Not Affect Polyhedrin Expression and Localization

According to previous reports, *ac75* is essential in the life cycle of the virus but deleting *ac75* did not affect viral genome replication (Guo et al., 2017; Shi et al., 2017). To investigate whether the AC75-F54S mutation affected transcription of viral genes, five viral genes, including two early genes (*iel* and *pe38*), one early-late gene (*gp64*) and two late genes (*vp39* and *polh*), were selected and analyzed. The transcript levels of the selected genes were determined by RT-qPCR with the corresponding primers (sequences are shown in **Table 1**). As shown in **Figure 6A**, no significant differences in transcript levels of all selected



genes were observed between vAc^{ac75F54S}-*ph*- and vAc^{ac75REP}-*ph*-transfected cells ($P > 0.05$). The results showed that the AC75-F54S mutation did not affect early or late viral gene transcription.

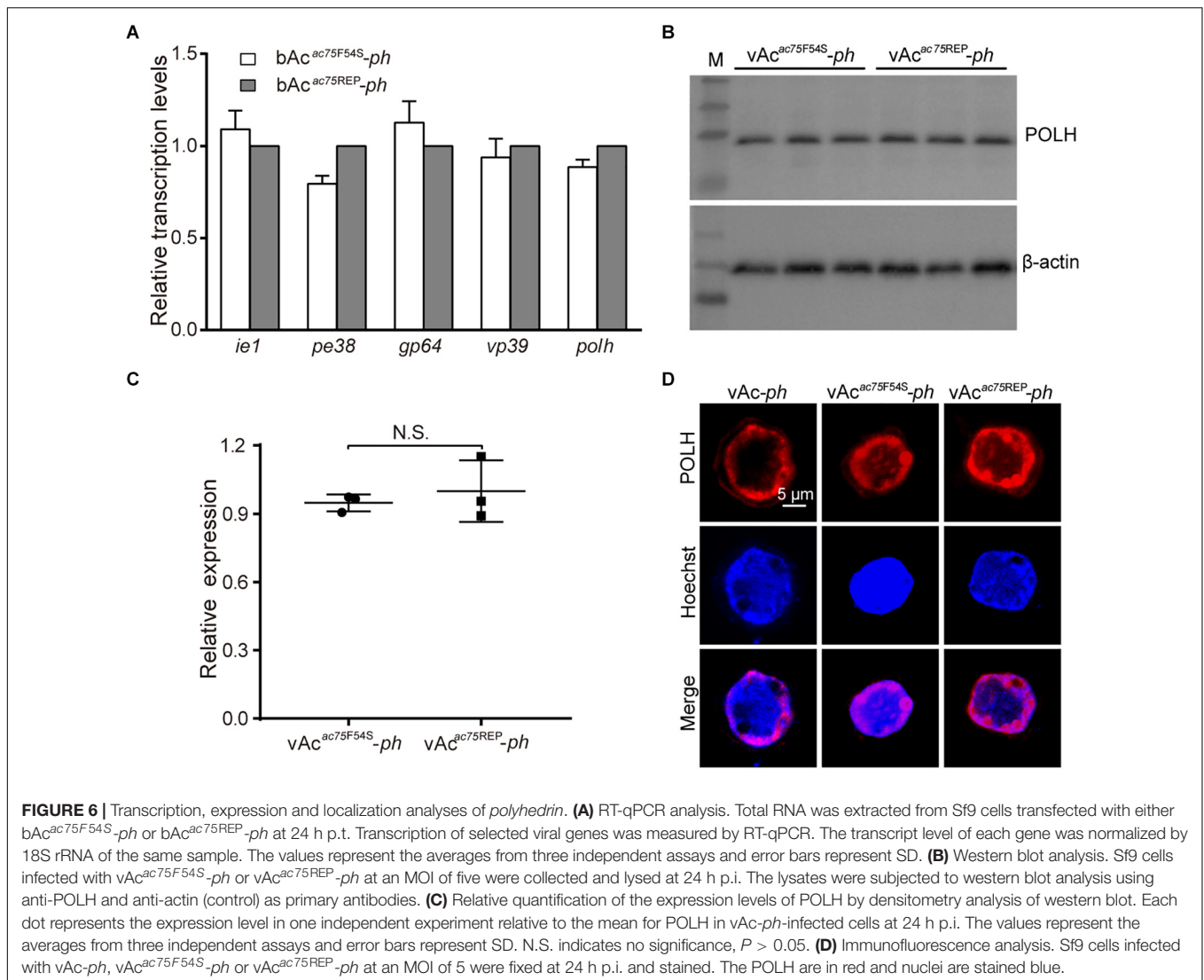
Western blot analysis was performed to determine whether the AC75-F54S mutation affected expression of the polyhedrin protein because the AC75-F54S mutation was found to impair OB formation. At 24 h p.i., there were no difference among the polyhedrin expression levels of vAc^{ac75F54S}-*ph*- and vAc^{ac75REP}-*ph*-infected cells (Figures 6B,C), indicating that the AC75-F54S mutation also did not affect polyhedrin expression. Furthermore, an immunofluorescence assay was performed to investigate the effect of the AC75-F54S mutation on polyhedrin localization. As shown in Figure 6D, polyhedrins were distributed predominantly in the nucleus, exhibiting a ring pattern in the ring zone, with a weak distribution in the cytoplasm of vAc-*ph*, vAc^{ac75F54S}-*ph*- and vAc^{ac75REP}-*ph*-infected cells at 24 h p.i. The results indicated that the AC75-F54S mutation did not affect the localization of the polyhedrin. Taken together, these data suggested that the AC75-F54S mutation might impair OB formation by affecting polyhedrin assembly.

The AC75-F54S Mutation Caused a Decreased in the Amount of AC75

To further investigate the nature of the defect caused by the AC75-F54S mutation, the relative protein expression levels of AC75 in vAc^{ac75F54S}-*ph*- or vAc^{ac75REP}-*ph*-infected cells were

compared over the course of infection by western blot analysis. As shown in Figures 7A, AC75 was detected in both vAc^{ac75F54S}-*ph*- and vAc^{ac75REP}-*ph*-infected cells at 18 and 24 h p.i.; however, the protein band representing AC75 in vAc^{ac75F54S}-*ph*-infected cells was much weaker in intensity when compared with that of vAc^{ac75REP}-*ph*-infected cells. The protein expression levels were further examined by standardization against actin expression and densitometry analysis. The relative AC75 protein expression in vAc^{ac75REP}-*ph*-infected cells was 0.58 ± 0.19 and 1.00 ± 0.16 at 18 and 24 h p.i., respectively (Figure 7B). In contrast, the relative AC75 protein expression in vAc^{ac75F54S}-*ph*-cells was 0.15 ± 0.07 and 0.41 ± 0.07 at 18 and 24 h p.i., respectively (Figure 7B). Immunoelectron microscopy analysis was performed with thin sections generated from cells infected with vAc-*ph*, vAc^{ac75F54S}-*ph* or vAc^{ac75REP}-*ph*, and fixed at 48 h p.i. In agreement with the above results, the number of colloidal-gold-labeled AC75 in the vAc^{ac75F54S}-*ph*-infected cells was remarkably lower when compared with that of vAc-*ph*- or vAc^{ac75REP}-*ph*-infected cells (Supplementary Figure 2).

Furthermore, immunofluorescence assays were performed to investigate the effect of the AC75-F54S mutation on the localization and abundance of AC75. At 15 h p.i., the AC75 signal was distributed uniformly throughout cells infected with vAc^{ac75F54S}-*ph* or vAc^{ac75REP}-*ph* (Figure 7C). By 24 and 48 h p.i., AC75 was localized predominantly within the nucleus, particularly around the nuclear rim and became condensed to



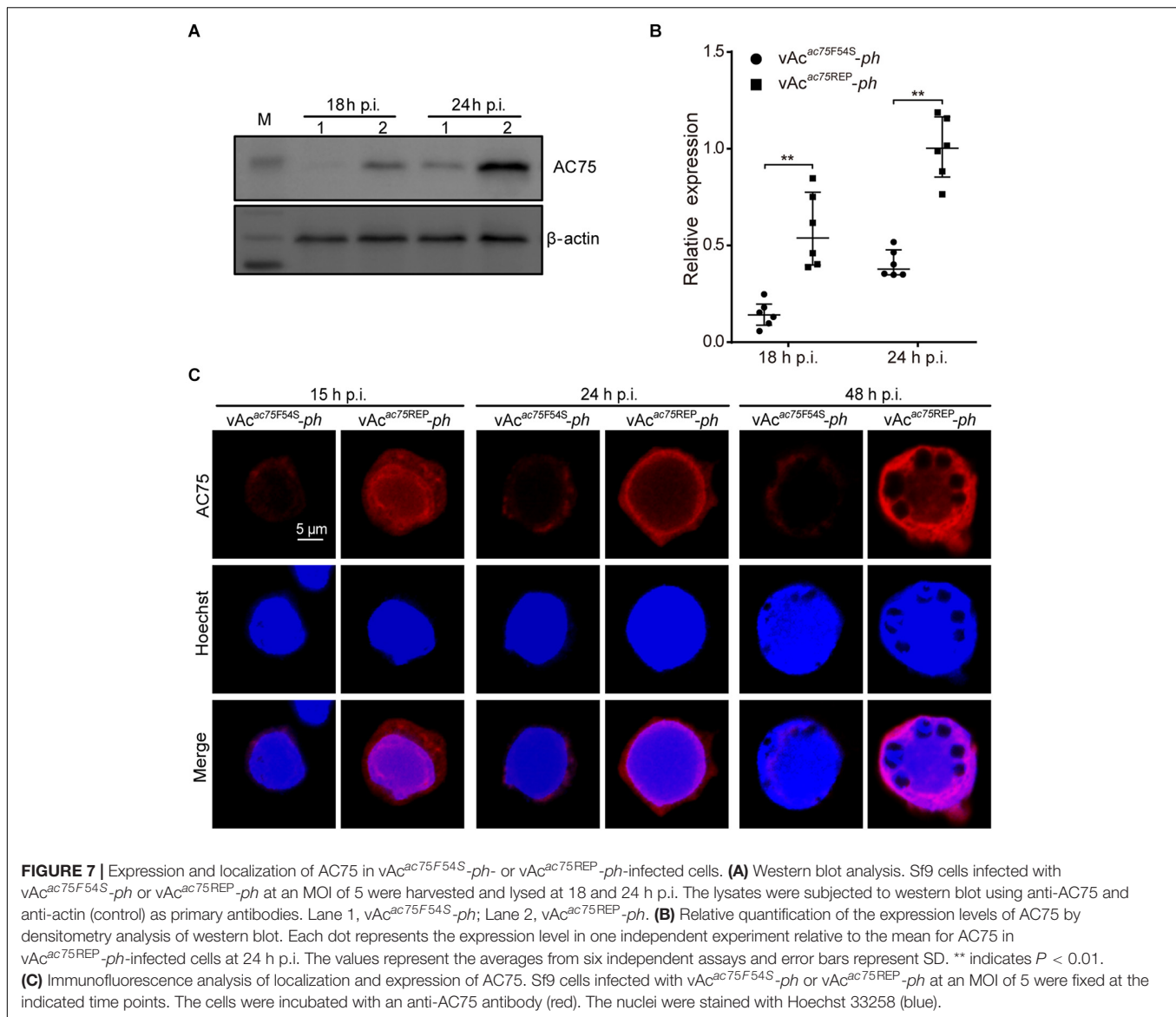
the intranuclear ring zone in $vAc^{ac75F54S-ph}$ - and $vAc^{ac75REP-ph}$ -infected cells (Figure 7C). Thus, the localization of AC75 was similar in $vAc^{ac75F54S-ph}$ - and $vAc^{ac75REP-ph}$ -infected cells. In contrast, the AC75 signal in $vAc^{ac75F54S-ph}$ -infected cells was much weaker when compared with those in $vAc^{ac75REP-ph}$ - and $vAc-ph$ -infected cells at all-time points (Figure 7C). The localization and abundance of AC75 in $vAc-ph$ -infected cells were comparable with those of $vAc^{ac75REP-ph}$ (Supplementary Figure 3). Taken together, these data demonstrated that the AC75-F54S mutation did not affect localization of AC75 in infected cells but caused a reduction in the amount of AC75.

The AC75-F54S Mutation Affected the Stability of AC75

The decrease in the amount of AC75 is probably because translation or stability of AC75 is affected by the AC75-F54S mutation. We initially examined and compared the expression of AC75 in cells transfected with $pIB-ac75^{F54S}egfp$ or $pIB-ac75egfp$

plasmids to determine whether the translation or the stability of AC75 was affected. The AC75 signal of cells transfected with $pIB-ac75^{F54S}egfp$ was much weaker than that of $pIB-ac75egfp$ with the same exposure time at 48 h p.t. (Figure 8A). Subsequently, we collected the cells and analyzed the mean fluorescence intensity of cells with EGFP by flow cytometry. As shown in Figure 8B, the mean fluorescence intensity of cells transfected with $pIB-ac75^{F54S}egfp$ was significantly lower than that of $pIB-ac75egfp$ ($P < 0.001$). These results indicated that the AC75-F54S mutation might impair AC75 stability.

To confirm the above results, a cycloheximide (CHX) treated assay was used to evaluate the relative stability of AC75. Briefly, Sf9 cells infected with $vAc^{ac75F54S-ph}$ or $vAc^{ac75REP-ph}$ at an MOI of five were treated with 400 $\mu\text{g/mL}$ CHX to block protein synthesis at 24 h p.i. The cells were collected and lysed at 0, 3, 6 and 12 h after CHX treatment, and the lysates were analyzed by western blot. The AC75 protein level in $vAc^{ac75F54S-ph}$ -infected cells was reduced significantly from 0 to 12 h (Figure 8C). In contrast, there were no obvious changes in AC75 protein



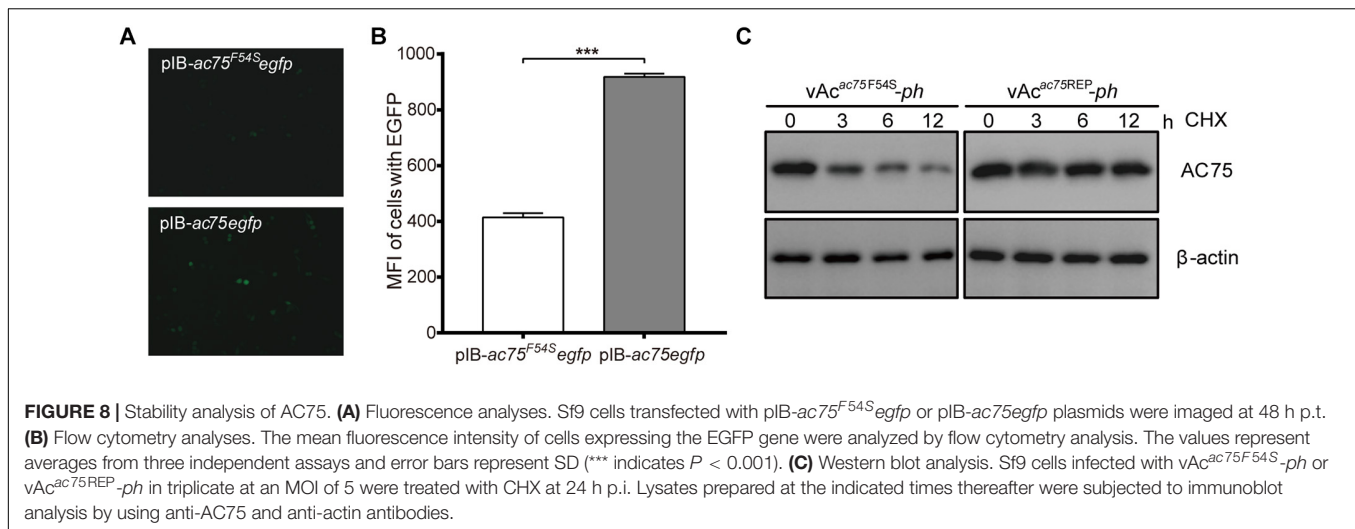
levels in vAc^{ac75REP}-ph-infected cells following CHX treatment (Figure 8C). Accordingly, these data are consistent with the flow cytometry results presented above. Taken together, these data suggest that the AC75-F54S mutation affects the relative stability of AC75 in infected cells.

DISCUSSION

ac75 is a highly conserved gene in all sequenced baculovirus genomes except CuniNPV. According to previous reports, *ac75* is essential for nuclear egress and intranuclear microvesicle formation (Guo et al., 2017; Shi et al., 2017). Deletion of *ac75* resulted in a complete loss of viral growth in cultured cells, which precluded the investigation of AC75 function during late infection. In this study, we identified that Phe-54 was an important

residue of AC75, and validated the important role of *ac75* in polyhedrin assembly and ODV embedding during OB formation.

Previous transcriptome analysis identified three typical late promoters located at 282, 93, and 14 nt upstream of the *ac75* start codon in *Trichoplusia ni* (*T. ni*) cells infected with AcMNPV (Chen et al., 2013). In this study, the transcription pattern revealed that *ac75* was transcribed from 12 h p.i. and this transcription persisted up to 72 h p.i. These observations are in accord with previous results showing that *ac75* was expressed at relatively high levels from 18 to 72 h p.i. in the AcMNPV-infected midgut of *T. ni* (Shrestha et al., 2018). In addition, western blot analysis revealed that AC75 was expressed during the late infection phase. Thus, *ac75* may play a role during the late stage of infection. Shi et al. (2017) and Guo et al. (2017) found that *ac75* was essential for nuclear egress and intranuclear microvesicle formation. However, the possible functions of *ac75*



in other processes during the late infection phase have not been investigated in detail.

Sequence alignment of AC75 homologs showed that Phe-54 and Gln-81 were completely conserved among the selected homologs. Phe is a hydrophobic amino acid with an aromatic side chain, whereas Gln has a polar, non-charged side chain. In this study, Phe-54 was mutated to glycine (F54G), alanine (F54A), or serine (F54S). These mutant viruses were transfected/infected into Sf9 cells, revealing that the AC75-F54S mutation produced 10-fold fewer progeny BVs than the wild-type virus, whereas the AC75-F54G mutation exhibited a modest two-fold reduction in viral titer when compared with that of the wild-type virus. The AC75-F54A mutation did not affect BV production (data not shown). Mutation of Gln-81 to glycine (Q81G), alanine (Q81A) or glutamic acid (Q81E) did not affect viral propagation (data not shown), indicating that residue Gln-81 may not be important for the functions of AC75. Thus, Phe-54 may be an important residue of AC75, and the AC75-F54S mutant virus was chosen for subsequent research.

In this study, novel functions of AC75 were investigated through characterization of the AC75-F54S partial loss-of-function mutant virus during the late infection phase. Electron microscopy revealed that the OBs of vAc^{ac75^{F54S}-ph} had a ragged surface and contained markedly low numbers of ODVs and most OBs of the vAc^{ac75^{F54S}-ph} were empty. In addition, the AC75-F54S mutation did not affect expression and localization of the polyhedrin. Thus, ac75 may play a key role in the assembly of the polyhedrin and the embedding of ODVs during OB morphogenesis. The process of OB occlusion requires a complex integration of events, including envelopment of ODVs, polyhedrin assembly and incorporation of ODVs. The mature ODVs associate with dense concentrations of the polyhedral protein, which subsequently crystallizes around one or many ODVs to form OBs. The mechanisms that control crystallization at the ODV-polyhedrin interface are unresolved and the viral proteins required for this process are unknown. The surface layer (calyx or polyhedral envelope) of mature OBs is composed of carbohydrates and PEP (Whitt and Manning, 1988). The

formation of this layer structure requires a functional P10 and is associated with nuclear fibrillar structures (Carpentier et al., 2008). The OBs of a pep or p10 mutant virus are irregular and fragile with no outer layer (Vlak et al., 1988; Li et al., 2015). According to recent reports, the OB morphology was also abnormal in a P33 point mutation and a VP91 truncated mutation (Kuang et al., 2017; Zhou et al., 2019), suggesting that both P33 and VP91 are involved in OBs morphogenesis, which involves assembly of the polyhedrin and the embedding of ODVs. Therefore, ac75 is the third gene identified to be involved with the assembly of the polyhedrin and embedding of ODVs. Further studies examining genes associated with OB formation will aid our understanding of this molecular mechanism.

Further investigation revealed that the AC75-F54S mutation reduced the amount of AC75, but did not affect localization in infected cells. We hypothesized that the lower amount of AC75 in vAc^{ac75^{F54S}-ph}-infected cells affected the efficiency of nuclear egress and therefore resulted in lower amounts of BV production. Flow cytometry and western blot analyses revealed that the lower levels of AC75-F54S might be a result of impaired stability caused by AC75-F54S mutation. The loss of persistence of AC75 may be caused by structural disorder. Thus, the AC75-F54S mutation may have caused mis-folding of AC75, which further affected its proper functions in the AcMNPV life cycle. Moreover, incorrectly folded AC75 may be degraded by the 20S proteasome (Asher et al., 2006; Tompa et al., 2008). Further analysis is required to determine the exact functional role of Phe-54 in AC75 activity in AcMNPV-infected cells.

In conclusion, we revealed that the residue Phe-54 in AC75 is important for the proper folding of this protein, and AC75 is involved in polyhedrin assembly and ODV embedding during OB formation. Thus, ac75 is a versatile gene associated with nuclear egress of nucleocapsids and OB morphogenesis. Moreover, our results provide evidence for a pivotal role of ac75 in BV production and OB formation, and further studies of AC75 are required to elucidate the relation between BV formation and OB morphogenesis. These data may help uncover the mechanism of OB morphogenesis of baculoviruses.

DATA AVAILABILITY STATEMENT

The datasets presented in this study can be found in online repositories. The names of the repository/repositories and accession number(s) can be found in the article/**Supplementary Material**.

ETHICS STATEMENT

The animal study was reviewed and approved by the Institutional Review Board, Wuhan Institute of Virology, Chinese Academy of Sciences.

AUTHOR CONTRIBUTIONS

XC, XS, and JH designed the experiments and wrote the manuscript. XC, XY, and CL carried out the experiments and analyzed the data. XC, JY, XS, and JH checked and finalized the manuscript. All authors contributed to manuscript revision, read, and approved the submitted version.

FUNDING

This work was supported by the National Key Research and Development Program of China (2018YFE0121900 to JH) and the WIV “One-Three-Five” strategic program (Y602111SA1 to XS). The funders had no role in study design, data collection, and interpretation, or the decision to submit the work for publication.

REFERENCES

- Asher, G., Reuven, N., and Shaul, Y. (2006). 20S proteasomes and protein degradation “by default”. *Bioessays* 28, 844–849. doi: 10.1002/bies.20447
- Ayres, M. D., Howard, S. C., Kuzio, J., Lopez-Ferber, M., and Possee, R. D. (1994). The complete DNA sequence of *Autographa californica* nuclear polyhedrosis virus. *Virology* 202, 586–605. doi: 10.1006/viro.1994.1380
- Biswas, S., Willis, L. G., Fang, M., Nie, Y., and Theilmann, D. A. (2017). *Autographa californica* Nucleopolyhedrovirus AC141 (Exon0), a Potential E3 Ubiquitin Ligase, Interacts with Viral Ubiquitin and AC66 To Facilitate Nucleocapsid Egress. *J. Virol.* 92, 01713–01717e.
- Blissard, G. W., and Theilmann, D. A. (2018). Baculovirus Entry and Egress from Insect Cells. *Annu. Rev. Virol.* 5, 113–139. doi: 10.1146/annurev-virology-092917-043356
- Blissard, G. W., and Wenz, J. R. (1992). Baculovirus gp64 envelope glycoprotein is sufficient to mediate pH-dependent membrane fusion. *J. Virol.* 66:6829.
- Braunagel, S. C., and Summers, M. D. (2007). Molecular biology of the baculovirus occlusion-derived virus envelope. *Curr. Drug Targets* 8, 1084–1095.
- Byers, N. M., Vandergaast, R. L., and Friesen, P. D. (2016). Baculovirus Inhibitor-of-Apoptosis Op-IAP3 Blocks Apoptosis by Interaction with and Stabilization of a Host Insect Cellular IAP. *J. Virol.* 90, 533–544. doi: 10.1128/JVI.02320-15
- Carpentier, D. C. J., Griffiths, C. M., and King, L. A. (2008). The baculovirus P10 protein of *Autographa californica* nucleopolyhedrovirus forms two distinct cytoskeletal-like structures and associates with polyhedral occlusion bodies during infection. *Virology* 371, 278–291.
- Chen, L., Hu, X., Xiang, X., Yu, S., Yang, R., and Wu, X. (2012). *Autographa californica* multiple nucleopolyhedrovirus odv-e25 (Ac94) is required for budded virus infectivity and occlusion-derived virus formation. *Arch. Virol.* 157, 617–625. doi: 10.1007/s00705-011-1211-9
- Chen, X., Yang, X., Lei, C., Qin, F., Sun, X., and Hu, J. (2020). *Autographa californica* Multiple Nucleopolyhedrovirus orf13 is Required for Efficient Nuclear Egress of Nucleocapsids. *Virol. Sin.* Preprint. doi: 10.1007/s12250-021-00353-3
- Chen, Y. R., Zhong, S., Fei, Z., Hashimoto, Y., Xiang, J. Z., Zhang, S., et al. (2013). The transcriptome of the baculovirus *Autographa californica* multiple nucleopolyhedrovirus in *Trichoplusia ni* cells. *J. Virol.* 87, 6391–6405. doi: 10.1128/JVI.00194-13
- Datsenko, K. A., and Wanner, B. L. (2000). One-step inactivation of chromosomal genes in *Escherichia coli* K-12 using PCR products. *Proc. Natl. Acad. Sci. U S A.* 97, 6640–6645. doi: 10.1073/pnas.120163297
- Fang, M., Dai, D., and Theilmann, D. A. (2007). *Autographa californica* multiple nucleopolyhedrovirus EXON0 (ORF141) is required for efficient egress of nucleocapsids from the nucleus. *J. Virol.* 81, 9859–9869.
- Gross, C. H., Russell, R. L., and Rohrmann, G. F. (1994). Orgyia pseudotsugata baculovirus p10 and polyhedron envelope protein genes: analysis of their relative expression levels and role in polyhedron structure. *J. Gen. Virol.* 75, 1115–1123. doi: 10.1099/0022-1317-75-5-1115
- Guo, Y. J., Fu, S. H., and Li, L. L. (2017). *Autographa californica* multiple nucleopolyhedrovirus ac75 is required for egress of nucleocapsids from the nucleus and formation of de novo intranuclear membrane microvesicles. *PLoS One* 12:e0185630. doi: 10.1371/journal.pone.0185630
- Hepp, S. E., Borgo, G. M., Ticau, S., Ohkawa, T., and Welch, M. D. (2018). Baculovirus AC102 Is a Nucleocapsid Protein That Is Crucial for Nuclear Actin Polymerization and Nucleocapsid Morphogenesis. *J. Virol.* 92, 111–118e. doi: 10.1128/JVI.00111-18

ACKNOWLEDGMENTS

We thank the Core Facility and Technical Support of Wuhan Institute of Virology, CAS, for the technical assistance in antibody preparation (Youling Zhu), fluorescence microscopy (Ding Gao and Juan Min) and electron microscope (Pei Zhang, Anna Du, and Bichao Xu).

SUPPLEMENTARY MATERIAL

The Supplementary Material for this article can be found online at: <https://www.frontiersin.org/articles/10.3389/fmicb.2021.663506/full#supplementary-material>

Supplementary Figure 1 | Sequence alignment of the AC75 homologs from 54 alphabaculoviruses and 12 betabaculoviruses. Amino acid sequences were aligned using Clustal X-2.0. Black shading denotes identical conserved residues, whereas gray shading indicates less conserved sites. Residues Phe-54 and Gln-81 were absolutely conserved among the selected homologs. The GenBank accession numbers of the amino acid sequences are presented in **Supplementary Table 1**.

Supplementary Figure 2 | Immunoelectron microscopy analysis. Sf9 cells were infected with vAc-ph, vAc^{act75F54S}-ph, or vAc^{act75REP}-ph at an MOI of five and harvested at 48 h p.i. Ultrathin sections were probed with the anti-AC75 antibody as the primary antibody and goat anti-rabbit IgG coated with gold particles (10 nm) as the secondary antibody.

Supplementary Figure 3 | Immunofluorescence analysis of localization and expression of AC75 in vAc-ph-infected cells. Sf9 cells were infected with vAc-ph (MOI = 5) and fixed at the indicated time points. The cells were incubated with an anti-AC75 antibody (red). The nuclei were stained with Hoechst 33258 (blue).

Supplementary Table 1 | The GenBank accession numbers of the amino acid sequences of AC75 homolog proteins selected in this study.

- Hodgson, J. J., Arif, B. M., and Krell, P. J. (2007). Reprogramming the χ Ia expression profile of *Autographa californica* multiple nucleopolyhedrovirus. *J. Gen. Virol.* 88(Pt 9), 2479–2487. doi: 10.1099/vir.0.82863-0
- Hu, Z., Yuan, M., Wu, W., Liu, C., Yang, K., and Pang, Y. (2010). *Autographa californica* multiple nucleopolyhedrovirus ac76 is involved in intranuclear microvesicle formation. *J. Virol.* 84, 7437–7447. doi: 10.1128/JVI.02103-09
- Ji, X., Zhang, C., Fang, Y., Zhang, Q., Lin, L., Tang, B., et al. (2015). Isolation and characterization of glacier VMY22, a novel lytic cold-active bacteriophage of *Bacillus cereus*. *Viral Sin.* 30, 52–58. doi: 10.1007/s12250-014-3529-4
- Jones, P., Binns, D., Chang, H. Y., Fraser, M., Li, W., McAnulla, C., et al. (2014). InterProScan 5: genome-scale protein function classification. *Bioinformatics* 30, 1236–1240. doi: 10.1093/bioinformatics/btu031
- Ke, J., Wang, J., Deng, R., and Wang, X. (2008). *Autographa californica* multiple nucleopolyhedrovirus ac66 is required for the efficient egress of nucleocapsids from the nucleus, general synthesis of preoccluded virions and occlusion body formation. *Virology* 374, 421–431. doi: 10.1016/j.virol.2007.12.033
- Kuang, W., Zhang, H., Wang, M., Zhou, N. Y., Deng, F., Wang, H., et al. (2017). Three Conserved Regions in Baculovirus Sulfhydryl Oxidase P33 Are Critical for Enzymatic Activity and Function. *J. Virol.* 91, 1158–1171. doi: 10.1128/JVI.01158-17
- Larkin, M. A., Blackshields, G., Brown, N. P., Chenna, R., McGettigan, P. A., McWilliam, H., et al. (2007). Clustal W and Clustal X version 2.0. *Bioinformatics* 23, 2947–2948. doi: 10.1093/bioinformatics/btm404
- Li, C., Wen, A., Shen, B., Lu, J., Huang, Y., and Chang, Y. (2011). FastCloning: a highly simplified, purification-free, sequence- and ligation-independent PCR cloning method. *BMC Biotechnol.* 11:92. doi: 10.1186/1472-6750-11-92
- Li, J., Zhou, Y., Lei, C., Fang, W., and Sun, X. (2015). Improvement in the UV resistance of baculoviruses by displaying nano-zinc oxide-binding peptides on the surfaces of their occlusion bodies. *Appl. Microbiol. Biotechnol.* 99, 6841–6853. doi: 10.1007/s00253-015-6581-6
- Li, Y., Shen, S., Hu, L., Deng, F., Vlak, J. M., Hu, Z., et al. (2018). The functional oligomeric state of tegument protein GP41 is essential for baculovirus BV and ODV assembly. *J. Virol.* 92, 2083–2017e.
- Marchler-Bauer, A., Bo, Y., Han, L., He, J., Lanczycki, C. J., Lu, S., et al. (2017). CDD/SPARCLE: functional classification of proteins via subfamily domain architectures. *Nucleic Acids Res.* 45, D200–D203. doi: 10.1093/nar/gkw1129
- McCarthy, C. B., Dai, X., Donly, C., and Theilmann, D. A. (2008). *Autographa californica* multiple nucleopolyhedrovirus ac142, a core gene that is essential for BV production and ODV envelopment. *Virology* 372, 325–339. doi: 10.1016/j.virol.2007.10.019
- Ohkawa, T., and Welch, M. D. (2018). Baculovirus Actin-Based Motility Drives Nuclear Envelope Disruption and Nuclear Egress. *Curr. Biol.* 28, 2153–2159. doi: 10.1016/j.cub.2018.05.027
- Qin, F., Xu, C., Hu, J., Lei, C., Zheng, Z., Peng, K., et al. (2019). Dissecting the Cell Entry Pathway of Baculovirus by Single-Particle Tracking and Quantitative Electron Microscopic Analysis. *J. Virol.* 93, 33–19e. doi: 10.1128/JVI.00033-19
- Qiu, J., Tang, Z., Cai, Y., Wu, W., Yuan, M., and Yang, K. (2019). The *Autographa californica* Multiple Nucleopolyhedrovirus ac51 Gene Is Required for Efficient Nuclear Egress of Nucleocapsids and Is Essential for In Vivo Virulence. *J. Virol.* 93, 1923–1918e. doi: 10.1128/JVI.01923-18
- Rohrmann, G. F. (2019). *Baculovirus Molecular Biology*, 4th Edn. Bethesda, MD: National Center for Biotechnology Information.
- Russell, R. L. Q., and Rohrmann, G. F. (1990). A baculovirus polyhedron envelope protein: Immunogold localization in infected cells and mature polyhedra. *Virology* 174, 177–184.
- Shi, A., Hu, Z., Zuo, Y., Wang, Y., Wu, W., Yuan, M., et al. (2017). *Autographa californica* Multiple Nucleopolyhedrovirus ac75 Is Required for the Nuclear Egress of Nucleocapsids and Intranuclear Microvesicle Formation. *J. Virol.* 92, 01509–01517e.
- Shorey, H. H., and Hale, R. L. (1965). Mass-Rearing of the Larvae of Nine Noctuid Species on a Simple Artificial Medium. *J. Econ. Entomol.* 58, 522–524.
- Shrestha, A., Bao, K., Chen, Y. R., Chen, W., Wang, P., Fei, Z., et al. (2018). Global Analysis of Baculovirus *Autographa californica* Multiple Nucleopolyhedrovirus Gene Expression in the Midgut of the Lepidopteran Host *Trichoplusia ni*. *J. Virol.* 92, 1277–1218e. doi: 10.1128/JVI.01277-18
- Tao, X. Y., Choi, J. Y., Kim, W. J., An, S. B., Liu, Q., Kim, S. E., et al. (2015). *Autographa californica* multiple nucleopolyhedrovirus ORF11 is essential for budded-virus production and occlusion-derived-virus envelopment. *J. Virol.* 89, 373–383. doi: 10.1128/JVI.01742-14
- Tao, X. Y., Choi, J. Y., Kim, W. J., Lee, J. H., Liu, Q., Kim, S. E., et al. (2013). The *Autographa californica* multiple nucleopolyhedrovirus ORF78 is essential for budded virus production and general occlusion body formation. *J. Virol.* 87, 8441–8450. doi: 10.1128/JVI.01290-13
- Tomba, P., Prilusky, J., Silman, I., and Sussman, J. L. (2008). Structural disorder serves as a weak signal for intracellular protein degradation. *Proteins* 71, 903–909. doi: 10.1002/prot.21773
- van Oers, M. M., and Vlak, J. M. (2007). Baculovirus genomics. *Curr. Drug Targets* 8, 1051–1068.
- Vlak, J. M., Klinkenberg, A. F., Zaal, K. J. M., Usmany, M., Klinge-Roode, E. C., Geervliet, J. B. F., et al. (1988). Functional Studies on the p10 Gene of *Autographa californica* Nuclear Polyhedrosis Virus Using a Recombinant Expressing a p10- β -Galactosidase Fusion Gene. *J. General Virol.* 69(Pt 4), 765.
- Wang, Y., Cai, Q., Chen, J., Huang, Z., Wu, W., Yuan, M., et al. (2019). *Autographa californica* Multiple Nucleopolyhedrovirus P48 (Ac103) Is Required for the Efficient Formation of Virus-Induced Intranuclear Microvesicles. *Viral Sin.* 34, 712–721. doi: 10.1007/s12250-019-00147-8
- Whitt, M. A., and Manning, J. S. (1988). A phosphorylated 34-kDa protein and a subpopulation of polyhedrin are thiol linked to the carbohydrate layer surrounding a baculovirus occlusion body. *Virology* 163, 33–42.
- Williams, G. V., Rohel, D. Z., Kuzio, J., and Faulkner, P. (1989). A cytopathological investigation of *Autographa californica* nuclear polyhedrosis virus p10 gene function using insertion/deletion mutants. *J. General Virol.* 70(Pt 1), 187.
- Xu, C., Wang, J., Yang, J., Lei, C., Hu, J., and Sun, X. (2019). NSP2 forms viroplasm during *Dendrolimus punctatus* cytopovirus infection. *Virology* 533, 68–76. doi: 10.1016/j.virol.2019.05.005
- Young, J. C., MacKinnon, E. A., and Faulkner, P. (1993). The Architecture of the Virogenic Stroma in Isolated Nuclei of Spodoptera frugiperda Cells in Vitro Infected by *Autographa californica* Nuclear Polyhedrosis Virus. *J. Struct. Biol.* 110, 141–153. doi: 10.1006/jsbi.1993.1015
- Yuan, M., Huang, Z., Wei, D., Hu, Z., Yang, K., and Pang, Y. (2011). Identification of *Autographa californica* nucleopolyhedrovirus ac93 as a core gene and its requirement for intranuclear microvesicle formation and nuclear egress of nucleocapsids. *J. Virol.* 85, 11664–11674.
- Yuan, M., Wu, W., Liu, C., Wang, Y., Hu, Z., Yang, K., et al. (2008). A highly conserved baculovirus gene p48 (ac103) is essential for BV production and ODV envelopment. *Virology* 379, 87–96. doi: 10.1016/j.virol.2008.06.015
- Yue, Q., Yu, Q., Yang, Q., Xu, Y., Guo, Y., Blissard, G. W., et al. (2018). Distinct Roles of Cellular ESCRT-I and ESCRT-III Proteins in Efficient Entry and Egress of Budded Virions of *Autographa californica* Multiple Nucleopolyhedrovirus. *J. Virol.* 92, 1636–1617e. doi: 10.1128/JVI.01636-17
- Zhou, F., Kuang, W., Wang, X., Hou, D., Huang, H., Sun, X., et al. (2019). The cysteine-rich region of a baculovirus VP91 protein contributes to the morphogenesis of occlusion bodies. *Virology* 535, 144–153. doi: 10.1016/j.virol.2019.06.016

Conflict of Interest: The authors declare that the research was conducted in the absence of any commercial or financial relationships that could be construed as a potential conflict of interest.

Copyright © 2021 Chen, Yang, Yang, Lei, Sun and Hu. This is an open-access article distributed under the terms of the Creative Commons Attribution License (CC BY). The use, distribution or reproduction in other forums is permitted, provided the original author(s) and the copyright owner(s) are credited and that the original publication in this journal is cited, in accordance with accepted academic practice. No use, distribution or reproduction is permitted which does not comply with these terms.